Scaling between stomatal size and density in forest plants

Congcong Liu[1,2#], Christopher D. Muir[3#], Ying Li[1], Li Xu[1], Mingxu Li[1], Jiahui Zhang[1,2], Hugo Jan de Boer[4], Lawren Sack[5], Xingguo Han[6], Guirui Yu[1,2], Nianpeng He[1,2,7*]

[1] Key Laboratory of Ecosystem Network Observation and Modeling, Institute of Geographic Sciences and Natural Resources Research, Chinese Academy of Sciences, Beijing 100101, China

[2] University of Chinese Academy of Sciences, Beijing 100049, China

[3] School of Life Sciences, University of Hawai'i at Mānoa, Honolulu, 96822, USA

[4] Copernicus Institute of Sustainable Development, Department of Environmental Sciences, Utrecht University, the Netherlands, 80125, Utrecht.

[5] Department of Ecology and Evolutionary Biology, University of California, Los Angeles, 90025, USA

[6] State Key Laboratory of Vegetation and Environmental Change, Institute of Botany, Chinese Academy of Sciences, Beijing 100093, China

[7] Institute of Grassland Science, Northeast Normal University, and Key Laboratory of Vegetation Ecology, Ministry of Education, Changchun 130024, China

[#] These authors contributed equally to this work.

*Corresponding author Nianpeng He (henp@igsnrr.ac.cn).

Tel.: +86-10-64889263

Fax: +86-10-64889399

Abstract

The size and density of stomatal pores limit the maximum rate of leaf carbon gain and water loss (g_{max}) in land plants. The limits of g_{max} due to anatomy, and its constraint by the negative correlation of stomatal size and density at broad phylogenetic scales, has been unclear and controversial. The prevailing hypothesis posits that adaptation to higher g_{max} is typically constrained by geometry and/or an economic need to reduce the allocation of epidermal area to stomata (stomatal-area minimization), and this would require the evolution of greater numbers of smaller stomata. Another view, supported by the data, is that across plant diversity, epidermal area allocated to guard cells versus other cells can be optimized without major trade-offs, and higher g_{max} would typically be achieved with a higher allocation of epidermal area to stomata (stomatal-area increase). We tested these hypotheses by comparing their predictions for the structure of the covariance of stomatal size and density across species, applying macroevolutionary models and phylogenetic regression to data for 2408 species of angiosperms, gymnosperms, and ferns from forests worldwide. The observed stomatal size-density scaling and covariance supported the stomatal-area increase hypothesis for high g_{max}. A higher g_{max} involves construction costs and maintenance costs that should be considered in models assessing optimal stomatal conductance for predictions of water use, photosynthesis, and water-use efficiency as influences on crop productivity or in Earth System models.

Stomatal pores are critical determinants of the function of plants and the composition of the atmosphere (1). The stomatal conductance to diffusion of water vapor and CO_2 (g_s) influences a broad spectrum of ecological processes at leaf, community, and ecosystem scales, including photosynthesis, net primary production, and water use efficiency (2, 3). Theoretically, stomata can regulate g_s through evolutionary or plastic shifts in stomatal size or numbers (4) or through short-term stomatal aperture changes (5). The g_s, and its typical operational value (g_{op}), can thus vary from near zero with stomata fully closed and g_{max} with stomata fully open. The g_{max} is a fundamental anatomical constraint, and across species measured under controlled conditions, g_{op} and g_{max} are correlated (6, 7). Because of their importance in controlling leaf water and CO_2 fluxes, stomatal anatomy can provide critical information in global vegetation and crop models (8-11) toward the current grand challenge of understanding how crops and forest trees are optimized for carbon gain versus water use. Yet, there has been substantial debate about the anatomical underpinnings of the evolution of higher g_{max}, and its associated costs.

The g_{max} is a mathematic function of underlying anatomical traits stomatal density (D_s, number of pores per unit epidermal area) and size (A_s, area of guard cells surrounding each pore). Indeed, these traits are widely used to study the adaptation and competition of plants because they are reliable indicators of g_{max}(12-18). Further an inverse relationship between A_s and D_s across diverse plant species has been recognized since 1865 (19). A prevalent view in the literature established by Franks and Beerling (20) is that the negative A_s and D_s relationship and the cost of stomatal area place a strong constraint on the evolution of g_{max}. According to an early version of the "stomatal area minimization hypothesis" a packing limit geometry constrains g_{max}, because the total fraction of epidermal area allocated to stomata (f_s) cannot exceed unity:

$$\boldsymbol{f_S = D_S A_S}. \qquad \textbf{(1)}$$

This, in turn generates the negative A_s and D_s relationship such that the evolution of larger numbers of stomata would necessitate reduction in their size. Thus, higher g_{max} can only be achieved by the evolution of larger numbers of smaller stomata. This early packing geometry argument was rendered moot given observations that for functional leaves, maximum f_s is usually far lower than unity (33.6% in our data; solid line in Fig. 1a). First, because stomata need to be spaced out by epidermal cells to open and close properly (21), and second, because the development of higher D_s can occur through the increased differentiation of epidermal cells into stomata (i.e., achieving higher stomatal differentiation rate, or stomatal index (22, 23), such that stomatal numbers can be independent of sizes. Yet the stomatal area minimization hypotheses for the evolution of higher g_{max} and its association with the negative A_s and D_s relationship was reached by a different argument: that to minimize stomatal construction and maintenance costs (24), plants evolving higher g_{max} must do so with a reduced f_s, and this maximization of g_{max} relative to f_s would in turn generate the negative A_s and D_s relationship (20).

To see why, note that a leaf's g_{max} is determined by stomatal anatomy:

$$g_{max} = bmD_S A_S^{0.5}, \quad (2)$$

where b and m are biophysical and morphological constants, respectively (22) (see Methods for equations to calculate these constants). By Eq. 2, a higher g_{max} can be achieved with a smaller total stomatal area by increasing stomatal number and reducing stomatal size, because smaller stomata also have a shorter channel for diffusion. For example, consider two leaves with stomatal densities 250 and 200 pores mm^{-2} and stomatal areas 150 μm^2 and 187.5 μm^2. They have identical f_S, but g_{max} at 25 °C is 11% greater for the leaf with smaller stomata (1.32 versus 1.47 mol m^{-2} s^{-1}). Thus, selection for higher g_{max} would result in more numerous, smaller

stomata, to minimize epidermal allocation to stomata and the evolution of higher g_{max} is strongly associated with the negative A_s and D_s relationship.

The 'stomatal-area minimization' hypothesis is controversial, however, as it is at odds with data in the literature that instead support an opposite, 'stomatal-area increase' hypothesis, i.e., that g_{max} should increase with f_S during evolution. Conversely, selection decreased g_{max} would be associated with decreased f_S. The positive covariance of g_{max} with f_S has been shown in many studies and has been utilized in many papers in the literature that have indeed used f_S as a proxy for g_{max} (25, 26). According to the "stomatal-area increase" hypothesis, selection for higher g_{max} is much stronger than that to minimize cost, leading to greater surface allocation, even if this incurs a cost. Under this scenario, the negative A_s and D_s relationship would not act directly as a constraint on g_{max}. Yet, selection for higher g_{max} would generate a distinctive covariation between these constituent anatomical traits. First, no relationship of A_s and D_s is absolutely required, which is consistent with data in the literature for species sets for which no relationship is found (27); as less than 50% of the leaf surface is typically taken up by stomata and many qualitatively different relationships between stomatal size and density across species are geometrically possible, including negative, zero, and positive covariances (ellipses in Fig. 1a). Yet, on average, a specific covariation would be expected if many combinations of A_s and D_s have similar fitness through their effect on either g_{max} or f_S, as we derive below.

It is critical to distinguish between these hypotheses for the evolution of g_{max} and the potential for f_S to constrain the observed stomatal size-density relationship. Implications of stomatal-area minimization are that g_{max} is ultimately constrained by the costs of high f_S, that such costs are minimized, and that evolving higher f_S would be slowed by costs associated with allocating too much epidermal area to stomata[27–32]. By contrast, the stomatal-area increase

hypothesis implies that selection on stomatal size and density primarily optimizes g_{max}, which varies across environments, and greater g_{max} incurs stomatal construction costs and opportunity costs of epidermal space. Testing these hypotheses will further reveal how the evolution of high g_{max} relates to the general inverse stomatal size-density relationship.

Indeed, these hypotheses can be tested against data for diverse species by considering in detail the covariation among D_S and A_S, for which they make different predictions. Under both hypotheses, D_S and A_S are constituents of composite traits, f_S or g_{max} (Eq. 1-2; Fig. 1b). We investigated how stomatal size-density scaling would differ between the hypotheses using models of macroevolutionary landscapes (28-31). We used the Ornstein-Uhlenbeck (OU) model originally derived from quantitative genetics for intraspecific (population) trait microevolution by Lande (32), and developed by Hansen (29)and others (28) for macroevolutionary interspecific trait variation. In the macroevolutionary OU model, interspecific trait variation expands through time until it reaches a stationary distribution around a long-term average(29). Within each species, microevolutionary forces (selection, genetic drift, mutation, and migration) and the environment drive genetic and plastic trait variation, respectively, and species' trait means should be near their current adaptive optimum. The across-species distribution that becomes stationary in the OU model is thus dependent on these independent shifts in species' optimum trait values. At stationarity, an OU process leads to stable trait mean and variance, setting the overall phenotypic constraint. Fitness tradeoffs likely limit the breadth of values for adaptive trait optima, given that extreme trait values will rarely optimize competing functions (33). Notably, the specific mechanisms for constraints on trait values are not specified but are implicit in the application of Ornstein-Uhlenbeck (OU) process to model evolution phenomenologically.

Given that the stomatal-area minimization and increase hypotheses differ in their prediction of how the species variation in composite traits (f_S and g_{max}) are constrained by their constituent traits (D_S and A_S), examination of the trait evolution can indicate which hypothesis was supported. The OU model can indicate *which* composite trait, f_S or g_{max}, is primarily constrained. In both cases, analogous quantitative theory shows that constraint on composite traits imposed by stabilizing selection limits variation in constituent traits(34), and constraint on f_S results in a different covariance structure of D_S versus A_S than a primary constraint on g_{max}. Note that both f_S and g_{max} show similar mathematical dependence on D_S and A_S:

$$\boldsymbol{Z_S = \lambda D_S A_S^{\beta}}, \quad \textbf{(3)}$$

where composite stomatal trait Z_S (i.e., f_S or g_{max}) is proportional to the product of constituent stomatal traits, with scaling exponent β multiplied by a scalar λ, which reflects stomatal dimension proportionalities and physical diffusion factors (22). For g_{max}, $\lambda = bm$ and $\beta = 0.5$ (Eq. 1); for f_S, $\lambda = 1$ and $\beta = 1$ (Eq. 2). Since all traits are log-normally distributed[31], and the OU model assumes Gaussian traits, we log-transformed Eq. 3:

$$\boldsymbol{z_S = \log(\lambda) + d_S + \beta a_S}, \quad \textbf{(4)}$$

where lowercase variables indicate log-transformation of uppercase counterparts. Log-transformation also has the advantage of simplifying variance decomposition by linearizing the equation and enables traits measured on different scales to be directly compared in their proportional changes. Using random variable algebra, the variance in z_S is defined as:

$$\mathrm{Var}(\boldsymbol{z_S}) = \mathrm{Var}(\boldsymbol{d_S}) + \boldsymbol{\beta^2}\mathrm{Var}(\boldsymbol{a_S}) + \boldsymbol{2\beta}\mathrm{Cov}(\boldsymbol{d_S}, \boldsymbol{a_S}). \quad \textbf{(5)}$$

Using the variance-covariance of d_S and a_S, we can find the scaling exponent β that minimizes $\mathrm{Var}(z_S)$:

$$\boldsymbol{\beta} = -\frac{\mathbf{Cov}(\boldsymbol{d}_S, \boldsymbol{a}_S)}{\mathbf{Var}(\boldsymbol{d}_S)} \quad \textbf{(6)}$$

Notably, the right-hand side of Eq. 6 is the negative of the ordinary linear regression slope of log-stomatal size against log-density. Thus, for any dataset, β can be estimated using ordinary regression methods, but a negative slope estimate will result in a positive value of $\hat{\beta}$. The stomatal-area minimization hypothesis predicts that $\hat{\beta} = 1$ because f_S constrains d_S and a_S (Eq. 1), whereas the stomatal-area increase hypothesis predicts that $\hat{\beta} = 0.5$ because g_{max} constrains d_S and a_S (Eq. 2). Note that the above prediction assumes that the primary constrained composite trait will also be the least variable composite trait, which allowed to identify the relationship between β and trait (co)variance in Eq. 6. We evaluated this assumption using forward-time, individual based, macroevolutionary quantitative genetic simulations (Supplementary Information). In each simulation, 1000 independent lineages evolve toward a moving optimal composite trait until stationarity following an OU process. The simulations confirm that the constrained composite trait is the least variable and that ordinary regression on interspecific trait means can accurately identify the simulated β. Estimates of β are not substantially affected by microevolutionary details about mutational and genetic covariances or geometric constraints on f_S (Fig. S2-S5).

We estimated stomatal size-density scaling in 2408 forest plant species from new field-collected samples over 28 sites in China and global synthesis of data from the literature (Fig. 2) and estimated the scaling exponent β using OU phylogenetic multiple regression with group (Angiosperm, Pteridophyte, Gymnosperm) and growth form (tree, shrub, herb) as covariates (see Methods).

Stomatal size-density scaling among forest plant species was consistent with a primary constraint on g_{max} (stomatal-area increase hypothesis, $\beta = 0.5$). Given the variance in stomatal

density, the covariance between size and density among forest species minimizes the variance in g_{max}. This implies that selection for higher g_{max} results in increased stomatal area allocation, and not minimizing area allocation (Fig. 3). There is no evidence that scaling differs between major groups, Angiosperms, Gymnosperms, and Pteridophytes (Fig. 3a; Table S1), but g_{max} is 49% (17-88% 95% CI; $P = 0.001$) and 14% (1-30% 95% CI; $P = 0.04$) higher in Angiosperms than Gymnosperms and Pteridophytes, respectively (Table S2). Trees also have 18% (8-28% 95% CI; $P < 0.0001$) and 48% (39-59% 95% CI; $P < 0.0001$) greater g_{max} than shrubs and herbs, respectively (Table S2). The across-species mean and variance in $\log(g_{max})$ are nearly invariant across latitude, temperature, and precipitation gradients, indicating that most of the variation in g_{max} occurs for species of contrasting ecology within rather than between forest sites, a finding similar to that for other key functional traits such as leaf mass per area and wood density (35) (Fig. 4).

Our results overturn the prevailing view that the evolution of high g_{max} across diverse species is constrained by size-density scaling and minimized stomatal area allocation. Instead, the covariance between stomatal size and density supports stomatal area allocation increasing with the evolution of high g_{max}. Thus, limits on the fraction of epidermis allocated to stomatal (f_S) are a secondary consequence of limits on g_{max}. Our novel analysis developed from quantitative genetic and macroevolutionary theory could distinguish the g_{max} evolution hypotheses. Notably, our β exponent for the scaling of d_S and a_S depends on using (phylogenetic) least squares regression, and thus, the results of studies reporting stomatal scaling slopes using standardized major axis (SMA) regression (which minimizes residual variance in both d_S and a_S) would need to be recalculated to test against our findings (see Supplementary Information). Although estimated scaling using standard phylogenetic regression approaches (see

196 Methods), it is more appropriate to interpret our results not as minimizing residual variance, but
197 rather estimating the β consistent with the covariance structure of stomatal size and density (Fig.
198 1).

199 Our results have at least two important implications for understanding the evolutionary
200 anatomical mechanisms of high g_{max} and its consequences for the stomatal size-density scaling
201 relationship. First, the finding that size-density scaling does not constrain the evolution of higher
202 g_{max} implies that stomatal cost is not a constraint on high g_{max} and thus a different constraint on
203 the evolution of extreme values of g_{max} across environments. Very high g_{max} may be rare because
204 the g_{op}:g_{max} ratio is constrained in a region of maximal control to respond rapidly to changing
205 environments (36). Additionally or alternatively, a high g_{max} may also be linked with a high
206 wilting point thereby setting a physical upper limit to leaf gas exchange and a high risk of
207 hydraulic failure (37) if open stomata face transiently high atmospheric drought. Other possible
208 costs include detrimental consequences of high g_{max} for stomatal movements and diffusion, as
209 well as energetic costs of opening closing more and/or larger stomata (38, 39). Future work
210 should prioritize identifying the fitness costs and functional trade-offs that constrain the
211 evolution of high g_{max}. Second, if g_{max} is the primary constraint, this implies that space allocation
212 to stomata is relatively unimportant, such that plants could allocate a greater fraction of their
213 epidermal area to stomata than they currently do without counterveiling selection. Thus, if
214 stomatal size and density can be manipulated independently, anatomies with the same g_{max}, but
215 different f_S, would have similar fitness in the same environment. This finding also clarifies the
216 evolution of stomata across major plant lineages, and refutes the hypothesis that smaller stomata
217 were required to increase g_{max} in angiosperms (20). All three major land plant lineages have
218 similar variance in g_{max} (Fig. 3b); angiosperms have higher g_{max} than gymnosperms and

pteridophytes on average due to their higher d_S for a given a_S, not because of differences in the scaling relationship. The higher stomatal density of angiosperms would be linked to increases in leaf water transport capacity, for example, by decreasing the distance between vein and stomata, allowing stomata to stay open[40]. The primary constraint on maximum stomatal conductance appears to be that selection rarely favors extreme values, implying that vegetation and crop models should incorporate nonepidermal costs of extreme trait values to predict optimal g_{max} for the prediction of photosynthetic carbon gain and transpiratory water loss across scales.

Methods

Stomatal trait data from global forests

The stomatal dataset of global forests represents a total of 2408 plant species from natural forests, including novel field data collected from Chinese forest communities and a compilation of published literature values.

Our field data were collected from 28 typical forest communities occurring between 18.7 °N and 53.3 °N latitude in China. The field sites were selected to cover most of the forest types in the northern hemisphere, including cold-temperate coniferous forest, temperate deciduous forest, subtropical evergreen forest, and tropical rain forest (Fig. 2). In total, we sampled 28 forest sites. We used the Worldclim database (40) to extract additional data on mean annual temperature (MAT) and precipitation (MAP) over the period 1960-1990 using latitude and longitude. Among these forests, mean annual temperature (MAT) ranged from -5.5-23.2 °C, and mean annual precipitation (MAP) varied from 320 to 2266 mm. The field investigation was conducted in July-August, during the peak period of growth for forests. Sampling plots were located within well-protected national nature reserves or long-term monitoring plots of field ecological stations, with relatively continuous vegetation. Four experimental plots (30 × 40 m) were established in each forest.

Leaves from trees, shrubs, and herbs were collected within and around each plot. For trees, mature leaves were collected from the top of the canopy in four healthy trees and mixed as a composite sample. Eight to 10 leaves from the pooled samples were cut into roughly 1.0 × 0.5 cm pieces along the main vein, and were fixed in formalin-aceto-alcohol (FAA) solution (5 ml 38 % formalin, 90 ml 75 % ethanol, 5 ml 100 % glacial acetic acid, and 5 ml 37 % methanol)

248 (41). In the laboratory, three small pieces were randomly sampled, and each replicate was
249 photographed twice using a scanning electron microscopy (Hitachi SN-3400, Hitachi, Tokyo,
250 Japan) on the lower surface at different positions. We focused on the lower epidermis (42),
251 because a previous study has demonstrated that most of leaf upper epidermis has no stomata for
252 forest plants (43).

253 In each photograph, the number of stomata was recorded, and D_S was calculated as the
254 number of stomata per unit leaf area. Simultaneously, five typical stomata were selected to
255 measure stomatal size using an electronic image analysis equipment (MIPS software, Optical
256 Instrument Co. Ltd., Chongqing, China).

257 Peer-reviewed papers on leaf stomata were collected using an all-databases search of Web
258 of Science (www.webofknowledge.com) from 1900 to 2018 using "forest" and "stomata" as a
259 topic, in line with the principle of "natural forest, non-intervention, species name" (i.e. we did
260 not use data from controlled experiments or where taxonomic data was missing). A total of 90
261 papers (see Supporting Table S3) which met our requirements, yielding D_S and L measurements
262 from 413 plant species (Fig. 2) from which we calculated g_{max} and f_S. f_S is proportional to the
263 stomatal pore area index (SPI), which defined as the product of D_S and stomatal length (L)
264 squared (25), because $A_S = mL^2$ (22).

265 We calculated g_{max} (Equation 1) to water vapor at a reference leaf temperature (T_{leaf} = 25°
266 C) following Sack and Buckley (22). They defined a biophysical and morphological constant as:

$$b = \frac{D_{WV}}{v}$$

$$m = \frac{\pi c^2}{j^{0.5}(4hj + \pi c)}$$

267 b is the diffusion coefficient of water vapor in air (D_{wv}) divided by the kinematic viscosity of dry
268 air (v). $D_{wv} = 2.49 \times 10^{-5}$ m^2 s^{-1} and $v = 2.24 \times 10^{-2}$ m^3 mol^{-1} at 25˚(44). For kidney-
269 shaped guard cells, $c = h = j = 0.5$; for dumbbell-shaped guard cells in the Poaceae, $c = h =$
270 0.5 and $j = 0.125$. We used the species average g_{max} and f_S for all analyses.

271 *Phylogenetic regression*

272 By positing that the least variable composite of stomatal size and density indicates the trait
273 with the most constraint (Fig. 1), we identify a new way to estimate the scaling exponent β (Eq.
274 6) using linear regression estimates, and also accounted for phylogenetic nonindependence. We
275 used the Plant List (http://www.theplantlist.org) to confirm species names, then we assembled a
276 synthetic phylogeny using S.PhyloMaker (45). We fitted phylogenetic regression models using
277 the **phylolm** version 2.6 package in R (46). As we derived in the main text, the scaling exponent
278 β can be estimated from the slope of the regression of a_S on d_S, where $\hat{\beta} = -\text{slope}$. We estimated
279 separate scaling exponents for major groups, Angiosperms, Pteridophytes, and Gymnosperms.
280 We also estimated different intercepts, corresponding with different average g_{max} values, for
281 functional types (herbs, shrubs, and trees) and grasses, because of their unique stomatal anatomy.
282 We used the "OUrandomRoot" model of trait evolution. 95% confidence intervals for all
283 parameters were estimated from 1000 parametric bootstrap samples generated by simulating
284 from the best-fit model and re-fitting. *P*-values for coefficients are based on *t*-tests. We used the
285 same methods to test whether g_{max} (log-transformed for homoskedasticity) was affected by
286 |latitude|, MAP, MAT, group (Angiosperms, Pteridophytes, Gymnosperms), and/or functional
287 type (herb, shrub, tree). One gymnosperm species, *Torreya fargesii*, had substantially lower
288 stomatal size than would be predicted from its density (Fig. 3a). There results of the paper did
289 not change if this outlier was excluded because the confidence intervals for stomatal-density

scaling are very wide for Gymnosperms regardless. Therefore, we excluded this species from statistical analyses but show it in the figure for completeness. All data were analyzed in R (47)version 4.0.5

297

298 # References

299 1. J. A. Berry, D. J. Beerling, P. J. Franks, Stomata: key players in the earth system, past
300 and present. *Current Opinion in Plant Biology* **13**, 232-239 (2010).
301 2. W. Cramer *et al.*, Global response of terrestrial ecosystem structure and function to CO_2
302 and climate change: results from six dynamic global vegetation models. *Global Change*
303 *Biology* **7**, 357-373 (2001).
304 3. M. Haworth, C. Elliott-Kingston, J. C. McElwain, Stomatal control as a driver of plant
305 evolution. *Journal of Experimental Botany* **62**, 2419-2423 (2011).
306 4. G. J. Jordan, R. J. Carpenter, A. Koutoulis, A. Price, T. J. Brodribb, Environmental
307 adaptation in stomatal size independent of the effects of genome size. *New Phytologist*
308 **205**, 608-617 (2015).
309 5. A. M. Hetherington, F. I. Woodward, The role of stomata in sensing and driving
310 environmental change. *Nature* **424**, 901-908 (2003).
311 6. P. J. Franks *et al.*, Sensitivity of plants to changing atmospheric CO_2 concentration: from
312 the geological past to the next century. *New Phytologist* **197**, 1077-1094 (2013).
313 7. M. Haworth, C. Elliott-Kingston, J. C. McElwain, Co-ordination of physiological and
314 morphological responses of stomata to elevated CO_2 in vascular plants. *Oecologia* **171**,
315 71-82 (2013).
316 8. J. C. Ordoñez *et al.*, A global study of relationships between leaf traits, climate and soil
317 measures of nutrient fertility. *Global Ecology and Biogeography* **18**, 137-149 (2009).
318 9. Z. Y. Yuan, H. Y. H. Chen, Global-scale patterns of nutrient resorption associated with
319 latitude, temperature and precipitation. *Global Ecology and Biogeography* **18**, 11-18
320 (2009).
321 10. S. Díaz *et al.*, The global spectrum of plant form and function. *Nature* **529**, 167-171
322 (2016).
323 11. G. T. Freschet *et al.*, Climate, soil and plant functional types as drivers of global fine-root
324 trait variation. *Journal of Ecology* **105**, 1182-1196 (2017).
325 12. H. T. Brown, F. Escombe, Static diffusion of gases and liquids in relation to the
326 assimilation of carbon and translocation in plants. *Proceedings of the Royal Society of*
327 *London* **67**, 124-128 (1901).
328 13. J.-Y. Parlange, P. E. Waggoner, Stomatal dimensions and resistance to diffusion. *Plant*
329 *Physiology* **46**, 337-342 (1970).
330 14. P. J. Franks, G. D. Farquhar, The effect of exogenous abscisic acid on stomatal
331 development, stomatal mechanics, and leaf gas exchange in *Tradescantia virginiana*.
332 *Plant Physiology* **125**, 935-942 (2001).
333 15. A. Vatén, D. C. Bergmann, Mechanisms of stomatal development: an evolutionary view.
334 *EvoDevo* **3**, 11 (2012).
335 16. J. C. McElwain, C. Yiotis, T. Lawson, Using modern plant trait relationships between
336 observed and theoretical maximum stomatal conductance and vein density to examine
337 patterns of plant macroevolution. *New Phytologist* **209**, 94-103 (2016).
338 17. M. À. Conesa, C. D. Muir, A. Molins, J. Galmés, Stomatal anatomy coordinates leaf size
339 with Rubisco kinetics in the Balearic *Limonium*. *AoB PLANTS* **12** (2019).

18. M. Murray *et al.*, Consistent relationship between field-measured stomatal conductance and theoretical maximum stomatal conductance in c3 woody angiosperms in four major biomes. *International Journal of Plant Sciences* **181**, 142-154 (2020).
19. A. G. Weiss, *Untersuchungen über die Zahlen-und Grössenverhältnisse der Spaltöffnungen* (Jahrbu¨cher fu¨r Wissenschaftliche Botanik, 1865), vol. 4.
20. P. J. Franks, D. J. Beerling, Maximum leaf conductance driven by CO_2 effects on stomatal size and density over geologic time. *Proceedings of the National Academy of Sciences* **106**, 10343-10347 (2009).
21. G. J. Dow, J. A. Berry, D. C. Bergmann, The physiological importance of developmental mechanisms that enforce proper stomatal spacing in Arabidopsis thaliana. *New Phytologist* **201**, 1205-1217 (2014).
22. L. Sack, T. N. Buckley, The developmental basis of stomatal density and flux. *Plant Physiology* **171**, 2358-2363 (2016).
23. E. J. Salisbury, On the causes and ecological significance of stomatal frequency, with special reference to the woodland flora. *Philosophical Transactions of the Royal Society of London Series B* **216**, 1-65 (1928).
24. R. M. Deans, T. J. Brodribb, F. A. Busch, G. D. Farquhar, Optimization can provide the fundamental link between leaf photosynthesis, gas exchange and water relations. *Nature Plants* **6**, 1116-1125 (2020).
25. L. Sack, P. D. Cowan, N. Jaikumar, N. M. Holbrook, The 'hydrology' of leaves: co-ordination of structure and function in temperate woody species. *Plant, Cell & Environment* **26**, 1343-1356 (2003).
26. S. F. Bucher *et al.*, Inter- and intraspecific variation in stomatal pore area index along elevational gradients and its relation to leaf functional traits. *Plant Ecology* **217**, 229-240 (2016).
27. Stephanie Dunbar-Co, Margaret J. Sporck, Lawren Sack, Leaf trait diversification and design in seven rare taxa of the hawaiian plantago radiation. *International Journal of Plant Sciences* **170**, 61-75 (2009).
28. M. W. Pennell, L. J. Harmon, An integrative view of phylogenetic comparative methods: connections to population genetics, community ecology, and paleobiology. *Annals of the New York Academy of Sciences* **1289**, 90-105 (2013).
29. T. F. Hansen, Stabilizing selection and the comparative analysis of adaptation. *Evolution* **51**, 1341-1351 (1997).
30. J. C. Uyeda, L. J. Harmon, A novel bayesian method for inferring and interpreting the dynamics of adaptive landscapes from phylogenetic comparative data. *Systematic Biology* **63**, 902-918 (2014).
31. F. C. Boucher, V. Démery, E. Conti, L. J. Harmon, J. Uyeda, A general model for estimating macroevolutionary landscapes. *Systematic Biology* **67**, 304-319 (2017).
32. R. Lande, Natural selection and random genetic drift in phenotypic evolution. *Evolution* **30**, 314-334 (1976).
33. L. Sack, T. N. Buckley, Trait multi-functionality in plant stress response. *Integrative and Comparative Biology* **60**, 98-112 (2019).
34. B. Walsh, M. W. Blows, Abundant Genetic Variation + Strong Selection = Multivariate Genetic Constraints: A Geometric View of Adaptation. *Annual Review of Ecology, Evolution, and Systematics* **40**, 41-59 (2009).

35. Mark Westoby, Daniel S. Falster, Angela T. Moles, a. Peter A. Vesk, I. J. Wright, Plant ecological strategies: Some leading dimensions of variation between species. *Annual Review of Ecology and Systematics* **33**, 125-159 (2002).
36. P. J. Franks, I. J. Leitch, E. M. Ruszala, A. M. Hetherington, D. J. Beerling, Physiological framework for adaptation of stomata to CO_2 from glacial to future concentrations. *Philosophical Transactions of the Royal Society B: Biological Sciences* **367**, 537-546 (2012).
37. C. Henry *et al.*, A stomatal safety-efficiency trade-off constrains responses to leaf dehydration. *Nature Communications* **10**, 3398 (2019).
38. H. J. de Boer *et al.*, Optimal allocation of leaf epidermal area for gas exchange. *New Phytologist* **210**, 1219-1228 (2016).
39. G. D. Farquhar, I. R. Cowan, E. Zeiger, *Stomatal Function*. G. D. Farquhar, I. R. Cowan, E. Zeiger, Eds. (Stanford University Press, Stanford, 1987), pp. 520.
40. R. J. Hijmans, S. E. Cameron, J. L. Parra, P. G. Jones, A. Jarvis, Very high resolution interpolated climate surfaces for global land areas. *International Journal of Climatology* **25**, 1965-1978 (2005).
41. N. He *et al.*, Variation in leaf anatomical traits from tropical to cold-temperate forests and linkage to ecosystem functions. *Functional Ecology* **32**, 10-19 (2018).
42. C. Liu *et al.*, Variation of stomatal traits from cold temperate to tropical forests and association with water use efficiency. *Functional Ecology* **32**, 20-28 (2018).
43. C. D. Muir, Light and growth form interact to shape stomatal ratio among British angiosperms. *New Phytologist* **218**, 242-252 (2018).
44. J. L. Monteith, M. H. Unsworth, "Chapter 2 - Properties of Gases and Liquids" in Principles of Environmental Physics (Fourth Edition), J. L. Monteith, M. H. Unsworth, Eds. (Academic Press, Boston, 2013), https://doi.org/10.1016/B978-0-12-386910-4.00002-0, pp. 5-23.
45. H. Qian, Y. Jin, An updated megaphylogeny of plants, a tool for generating plant phylogenies and an analysis of phylogenetic community structure. *Journal of Plant Ecology* **9**, 233-239 (2015).
46. L. Ho, C. Ané, A linear-time algorithm for Gaussian and non-Gaussian trait evolution models. *Syst Biol* **63**, 397-408 (2014).
47. R. C. Team (2021) R: A language and environment for statistical computing. Foundation for statistical computing. . in *R: A language and environment for statistical computing. Foundation for statistical computing.* (Vienna, Austria, Vienna, Austria).

Acknowledgements

Financial support was supported by the National Natural Science Foundation of China (31988102, 31770655, 31870437), the National Key R&D Program of China (2017YFA0604803), the second Tibetan Plateau Scientific Expedition and Research Program (2019QZK060202), The Chinese Academy of Sciences Strategic Priority Research Program (XDA23080401), US National Science Foundation 1929167 (to CDM), and the Project funded by China Postdoctoral Science Foundation (2020M680663). We thank "Functional Trait Database of Terrestrial Ecosystems in China (China_Trait)" for sharing data, further information for other materials should contact to N.P. He (henp@igsnrr.ac.cn). There are no conflicts of interest to declare.

Author contributions

N.H. and G.Y. designed field sampling; N.H., C.D.M, and C.L. conceived the initial ideas; C.L., N.H., Y.L. J.Z., Z.Z., M.L. and L.X collected the data; C.L. wrote the first draft, and C.D.M. contributed the final mathematical derivations, data analysis, and wrote the final manuscript; L.S., H.J.B., C.L., N.H., G.Y., and X.H. revised the manuscript. All authors gave final approval for publication.

Supplementary information

Figures

a **Many relationships between stomatal size and density are geometrically possible**

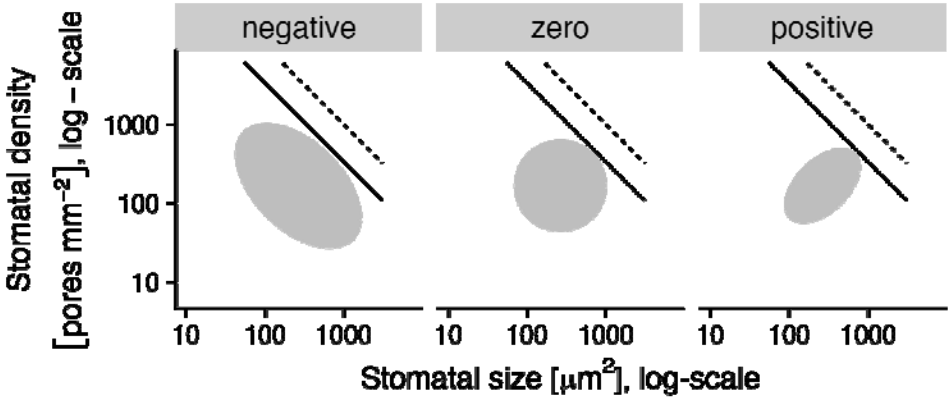

b **Hypothesis: covariation in stomatal size and density is shaped by constraint on a composite trait**

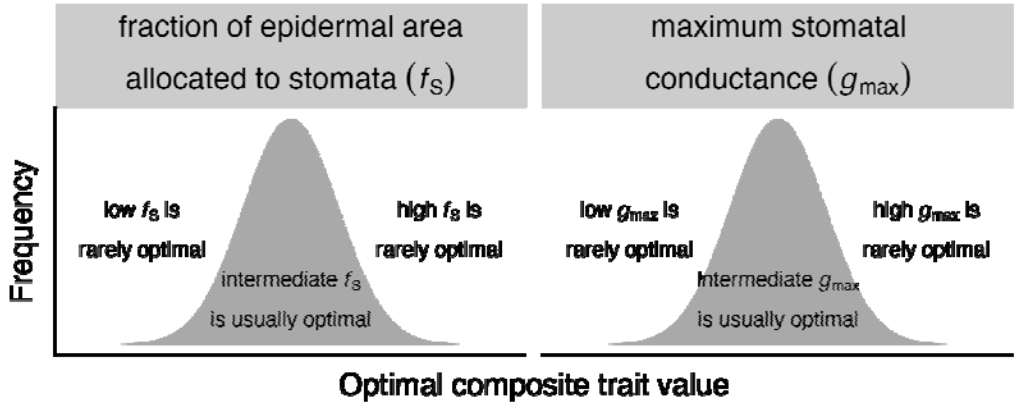

c **Prediction: stomatal size-density covariation depends on which composite trait is constrained**

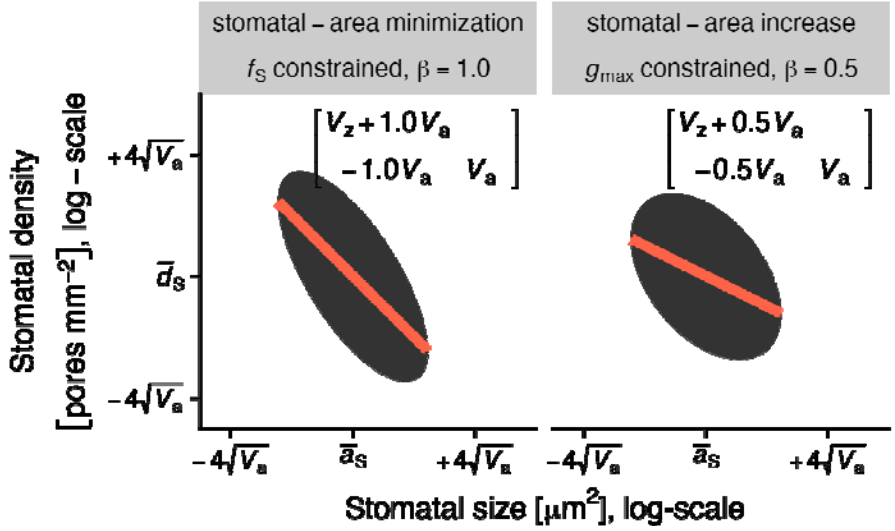

444

Fig. 1 | Competing hypotheses for stomatal size-density scaling make different predictions about the trait covariance structure. Maximum stomatal conductance (g_{max}) and the fraction of epidermal area allocated to stomata (f_S) are composite traits determined by stomatal density and size. On a log-scale, they are the sum of log-stomatal density (d_S) and log-stomatal size (a_S) times a scaling exponent (β), 0.5 for g_{max} and 1.0 for f_S (see Methods). **a**. Many scaling relationships between stomatal size and density are possible as long as f_S does not exceed 1 (dashed line) or more realistically a value less than 1 to allow space between stomata (solid line, f_S = 0.34, the maximum value in our data set). The grey ellipses represent different possible scaling relationships with the same mean trait values in our data set ($\bar{A}_S = 263\ \mu m^2$, $\bar{D}_S = 168\ pores\ mm^{-2}$). These are 95% quantile of covariance ellipses for a bivariate normal with trait correlations of -0.5, 0, and 0.5 and trait variances of 0.75, 0.55, and 0.45 for 'negative', 'zero', and 'positive' relationships, respectively. **b.** We hypothesized that size-density scaling is determined by constraint on either g_{max} (stomatal-area increase; left panel) or f_S (stomatal-area minimization; right panel). Under either hypothesis, the optimal composite trait varies but extreme values of the composite trait are rarely optimal. **c.** Both hypotheses predict negative size-density scaling but with different covariance relationships. If the interspecific means ($\bar{d}_S, \bar{a}_S$) and variances (V_d, V_a) of stomatal density and size, respectively, are measured, the covariance between them ($V_{d,a}$) is equal to -βV_a. Under the stomatal-area increase (left panel) and stomatal-area minimization (right panel) hypotheses, β should be 0.5 and 1, respectively. The ellipse is the 0.95 quantile of covariance ellipse associated with the covariance matrix (upper right corner of the plot); the orange line is the scaling exponent fit through the constituent trait means.

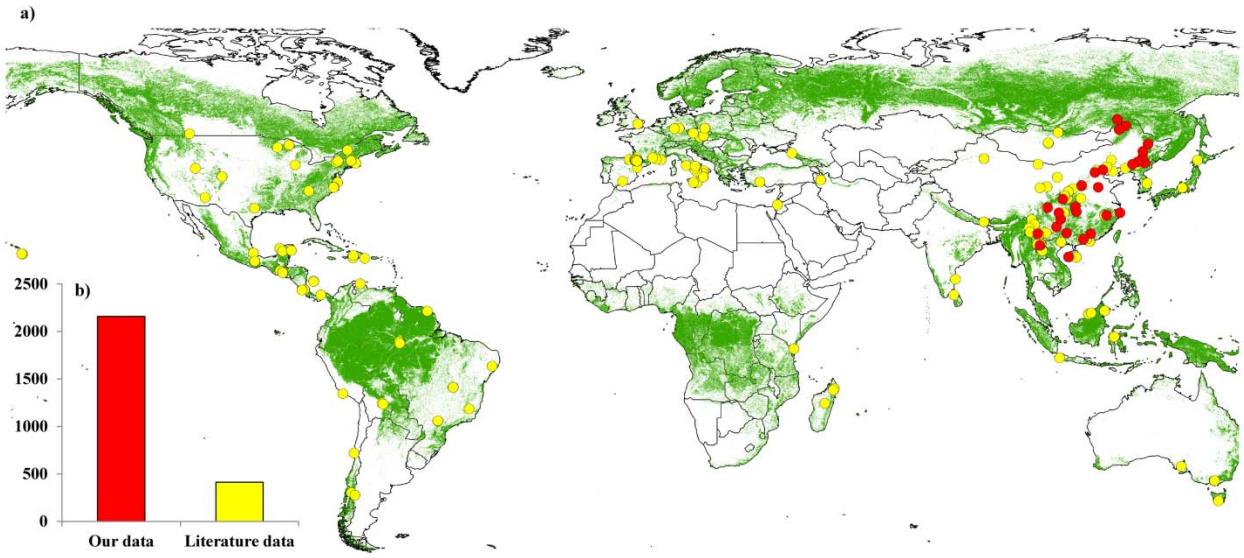

Fig. 2 | Geographic distribution of sampling sites (a) and the number of plant species (b) in this study.

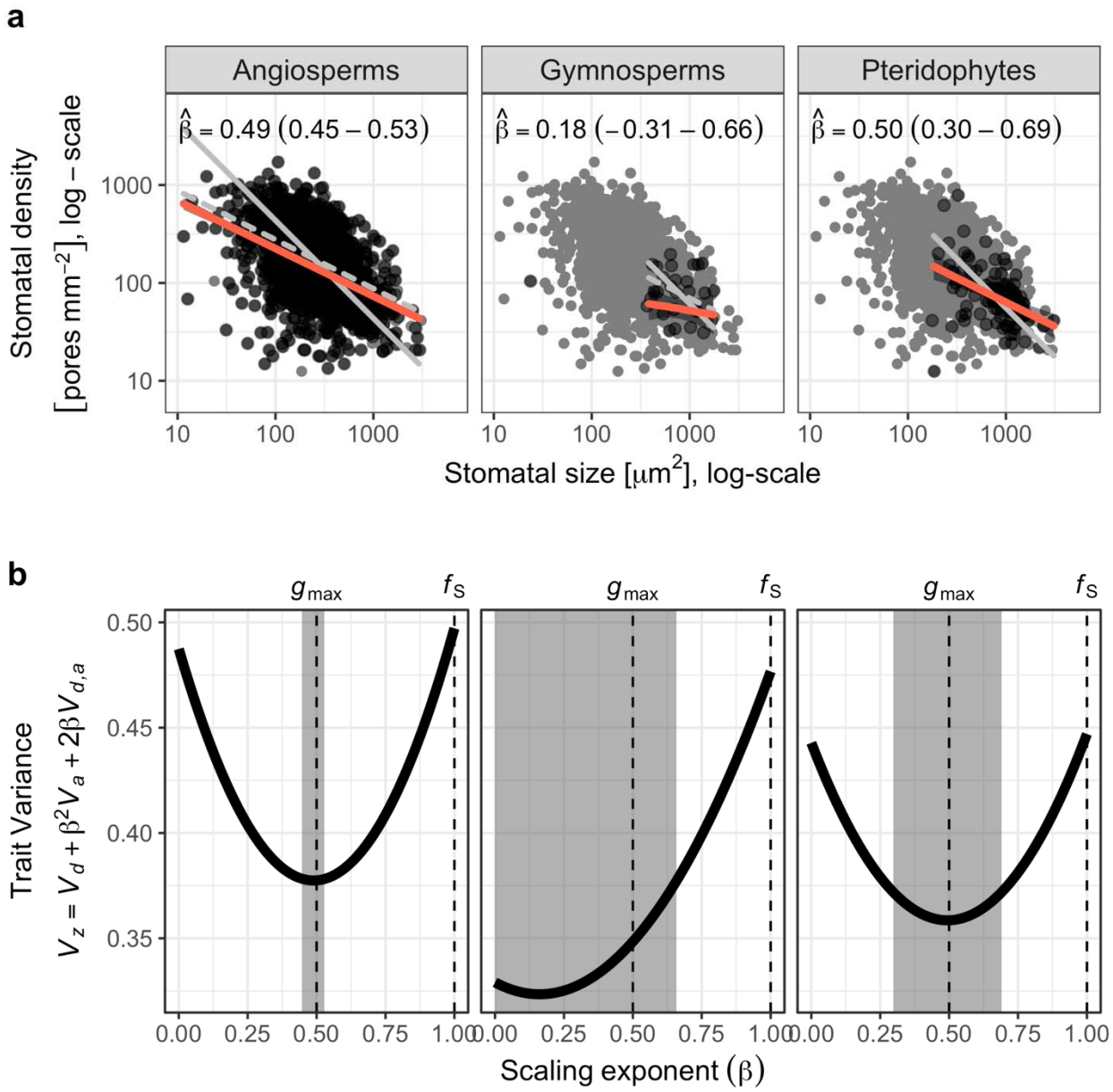

Fig. 3 | Stomatal size-density scaling is consistent with stomata-area increase but not area-minimization. a. In both angiosperms (left panel) and pteridophytes (right panel), the scaling exponent ( ) estimated as the phylogenetic linear regression slope of stomatal size against density (Methods) is close to 0.5 as predicted by the stomatal-area increase hypothesis, but much less than 1.0, as predicted by the stomatal-area minimization hypothesis. For comparison, thin gray lines in the background show predicted slopes for each group when = 1.0 (solid line) and

477 β = 0.5 (dashed line). The bootstrap 95% confidence intervals are in parentheses and shown
478 graphically by the width of the grey rectangle in **b**. Dark points represent species mean trait
479 values from the focal group; grey background points are from all groups for comparison. Orange
480 line and ribbon are the estimated phylogenetic regression line and the 95% bootstrap confidence
481 intervals. Scaling in gymnosperms (middle panel) is not significantly different from 0 or 0.5, but
482 the confidence intervals do not include 1.0. **b.** The variance of the composite trait (V_z) is
483 minimized near β = 0.5, as predicted under the stomatal-area increase hypothesis (dashed-line
484 under g_{max}) but not where β = 1.0 as predicted by the stomatal-area minimization hypothesis
485 (dashed-line under f_S).

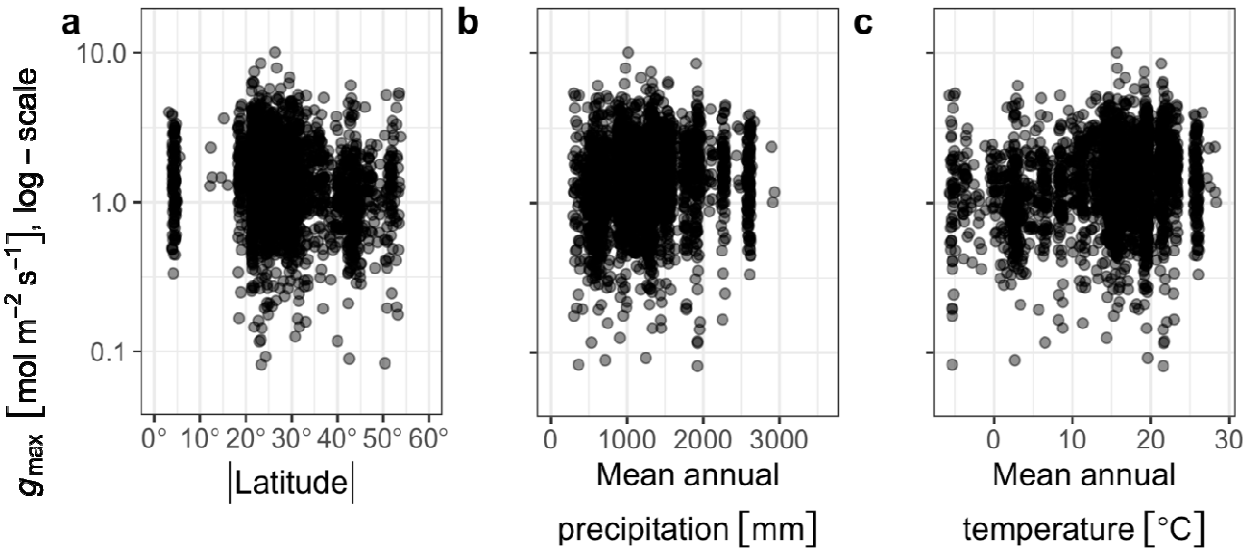

Fig. 4 | Anatomical maximum stomatal conductance varies little with latitude, mean annual precipitation, or mean annual temperature. Each point is the species' mean |latitude| (**a.**), mean annual precipitation (**b.**), or mean annual temperature (**c.**) on the *x*-axis and the maximum stomatal conductance (g_{max}) on the *y*-axis (log-scale). Based on phylogenetic multiple regression, the relationship between log(g_{max}) and mean |latitude| (P = 0.69) and mean annual temperature (P = 0.10) are not significant; the relationship with mean annual precipitation is significant (P = 0.009) but weak since the total model R^2 including all climate, lineage, and growth explanatory variables is only 0.11.